Design Aspects of High-Performance Indoor Optical Wireless Transceivers

Chaturi Singh*, Joseph John, Y.N.Singh and K.K.Tripathi

*National Wind Tunnel Facility, IIT Kanpur 208016, INDIA

Email: chaturi@iitk.ac.in

Abstract- **The ever-increasing use of portable computing and multimedia terminals in recent years has led to keen interests in the area of high-speed wireless digital links and local area networks. In indoor environments, optical wireless technology offers major performance advantages over radio and microwave technologies. But several aspects limit the performance of indoor optical wireless systems. Important ones being; eye safety problems, speed limitation of the optoelectronic devices, high path loss, multipath dispersion, and noise induced by natural and artificial light on the receiving photo diodes. This paper considers these system performance-limiting factors and presents the design aspects of eye-safe and high-performance indoor optical wireless link transmitters and receivers (transceivers) suitable for wireless local area networks.**

1. INTRODUCTION

The provision of voice, data, and visual communications to indoor mobile users in recent years has led to keen interests in the area of high-speed wireless digital links and local area networks (LANs). For indoor wireless connectivity, the market for radio frequency (RF) wireless networks is growing rapidly and data rates available with them are also rising. In spite of this, there is an increasing mismatch in the transmission data rate between fixed and mobile networks. Fiber optical LANs will be carrying traffic at data rates of tens of gigabits per second in the near future, whereas it will be difficult to provide even data rates of tens of megabits per second to mobile users. In this regime, the promise of high un-regulated bandwidth at a low-cost and low-power consumption makes optical wireless (OW), more specifically infrared (IR) communication an attractive technical alternative to the RF approach [1]. But several aspects limit the performance of indoor optical wireless systems. Important ones being; eye safety problems, speed limitation of the optoelectronic devices (LEDs and PIN photodiodes), high path loss, multipath dispersion, and noise induced by natural and artificial light on the receiving photo diodes [2]. This paper considers most of these system performance-limiting factors and discusses design techniques for the eye-safe, power-efficient and high-speed optical wireless transceivers. The optical links using these transceivers are well suited for wireless networking of stationary as well as portable computers and multimedia terminals within a room, and terminals on backbone.

2. TRANSCEIVER DESIGN ASPECTS

An indoor optical wireless link for LANs is shown in Fig. 1. The link is based on star network topology and has an active base station (BS) mounted on the ceiling of a room above the coverage area. To form a local area network, the BS as well as each terminal located in the coverage area is equipped with an integrated optical transceiver. The individual component of the transceiver consists of a light source, its paired detector and the necessary drive, amplifier, control and modulation or demodulation electronics as illustrated in Fig. 2. In the proposed transceivers, the tracking function is achieved by the combination of a multi-element transmitter and multi-element receiver. The preferred configuration for transmitter and receiver arrays would be hexagonal, but for reasons of availability, we have considered square arrays. The Ethernet MAC protocol can be used for the link transceivers since the base station on the ceiling establishes a shared medium.

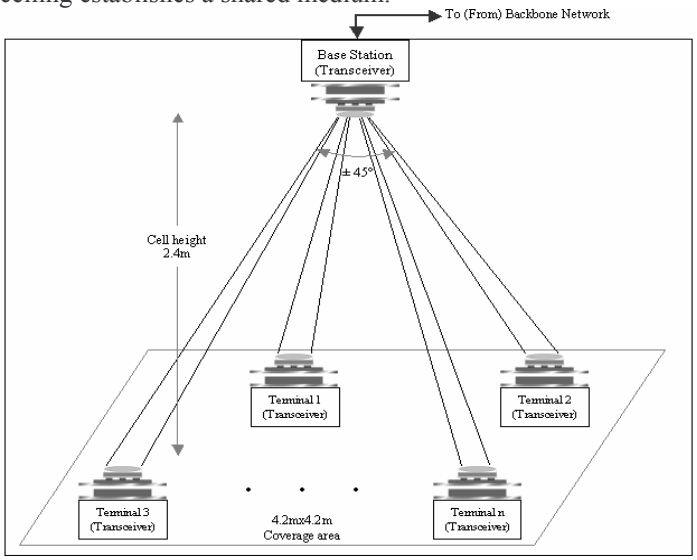

Fig. 1. An indoor optical wireless link for LANs.

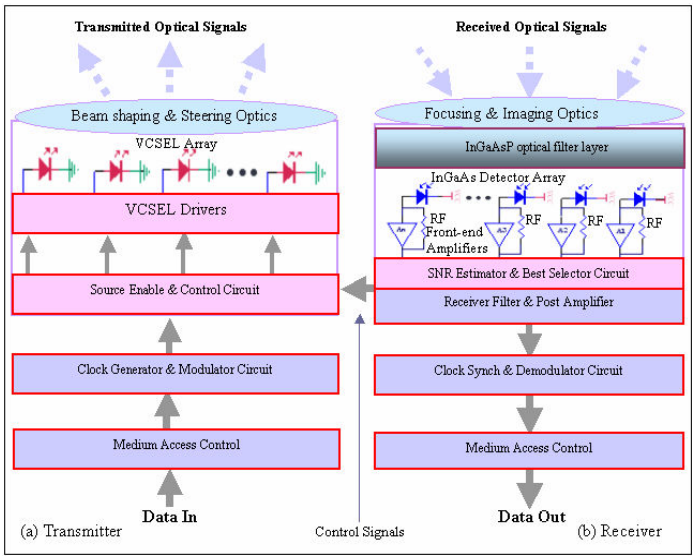

Fig. 2 Schematic of an indoor optical wireless transceiver.

2.1. System Configuration

There are three generic system configurations available for indoor optical wireless links, viz; directed beam infrared (DBIR), diffuse infrared (DFIR) and quasi-diffuse infrared (QDIR) or tracked [1, 2]. Out of them, tracked configuration used for this work shows superior performance in achieving high bit rate transmission and significant power margins. Owing to the highly directive nature of the link, large optical concentration ratios can be exploited. This also allows relatively small area detectors to be used, as it will be the concentrator area that collects the signal.

2.2. Selection of Transmission Wavelength

Currently, IR technology is designed for operation at 850nm wavelength [1], although the latest technology includes 1.55µm wavelength devices [3, 4]. The use of 1.55µm wavelength devices for the proposed transceivers is attractive due to the following reasons: Firstly, they cannot harm the human eye; the outer part of the human eye (cornea) filters incoming light and passes wavelengths ranging from 0.4µm to 1.4µm. Thus, transmissions at 1.55µm wavelength do not pass through the corneal filter, and cannot harm the sensitive retina. Secondly, at these wavelengths, the emitted power is permissible up to 10mW [5] (without exceeding the eye safety limits) and improves the available link power budget. Thirdly, the optical environment becomes progressively quieter with increasing wavelength [1, 2]. Thus, at these wavelengths, the system receivers are immune to strong ambient infrared radiation (except incandescent light sources).

2.3. Transmitter Design

Typically in an indoor optical wireless system while maintaining a high quality and reliable communication performance, the end terminals need to move freely within the room. This requires uniform optical power distribution in the receiver plane. This can be achieved using a multi-element transmitter, which emits multiple narrow beams. These types of transmitters are also expected to reduce the path loss compared to the diffuse transmitter, because the narrow beam experiences little path loss traveling from the transmitter to the destination receivers. The multi-element transmitter can be realized using two-dimensional (2-D) arrays of long wavelength vertical-cavity surface-emitting lasers (VCSELs) equipped with integrated circuit drivers [3, 4]. The use of VCSELs as light sources is considered due to their well-controlled narrow beam properties, high modulation bandwidth, low power consumption and the possibility of array arrangements. The transmitter projects an average light power of 10mW at 1.55µm wavelength in the form of multiple narrow beams to offer excellent power budget and make the link eye-safe and nearly immune to ambient light noise. The field of view (FOV) of the transmitter is set from ±45º to ±50º by using a 9x9 VCSEL array to achieve a sufficient coverage area in the receiver plane. To minimize the transmitted power, a source enable and control circuit of the transmitter as shown in Fig. 2(a) deactivates the VCSEL elements not emitting in directions of the destination receivers.

The VCSELs used for optical transmitter emit beams with a Gaussian intensity profile, which results in a non-uniform intensity distribution in the receiver plane. An exponential field distribution profile with order more than 2 (super-Gaussian) is expected to provide better intensity distribution. To achieve this, the non-uniform Gaussian beams produced by the transmitter can be passed through a beam shaping and steering optics to create a uniform flat-top intensity profile in the receiver plane. The beam shaping and steering optics can be realized using array-type diffractive elements (DEs) [6].

Transmitter Intensity Profile

The super-Gaussian (SG) intensity profile of a VCSEL beam is a function of axial and radial distances Z and r, respectively, and can be expressed as

$$I_{sg}(r) = I_{sg_0} e^{-2(r/w)^p} = P_T \frac{2^{2/p} \cdot p}{2\pi w^2 \Gamma(2/p)} e^{-2(r/w)^p} \qquad (1)$$

where p is the order of the SG profile, $w = w_z = \lambda.Z/\pi w_0$ is the radius of the $1/e^2$ contour after the beam has propagated a distance Z. P_T, λ and w_0 are the average power, wavelength and waist of the VCSEL beam, respectively. The Gaussian profile of the VCSEL beam is a special case SG-2 for $p=2$ in Eq. (1).

We have simulated far-field Gaussian and super-Gaussian intensity profiles (Fig. 3) for a 5x5 VCSEL array-based transmitter using LabVIEW graphical programming tool. For simulation, the parameters taken are; P_T = 10mW, λ = 1.55µm, w_0 = 4.25µm and Z = 2.4m.

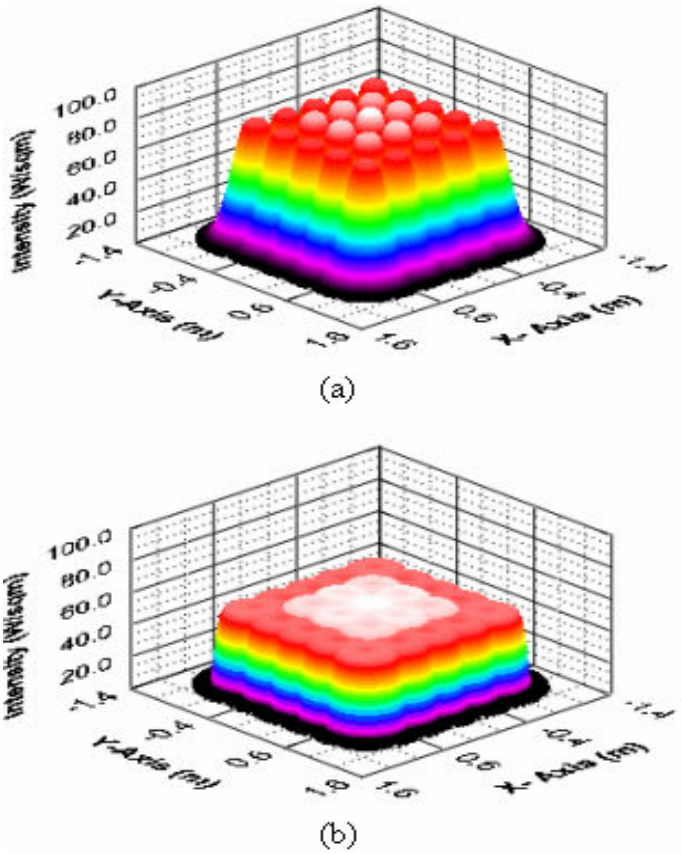

Fig. 3. Simulated intensity profile of a 5x5 VCSEL array-based transmitter; (a) Gaussian profile, and (b) super-Gaussian (flat-top) profile.

Fig. 4 shows the top view of the Gaussian profile cells in the receiver plane with one set of diagonal cells indicated as C2′d, C1′d, C0, C1d, and C2d.

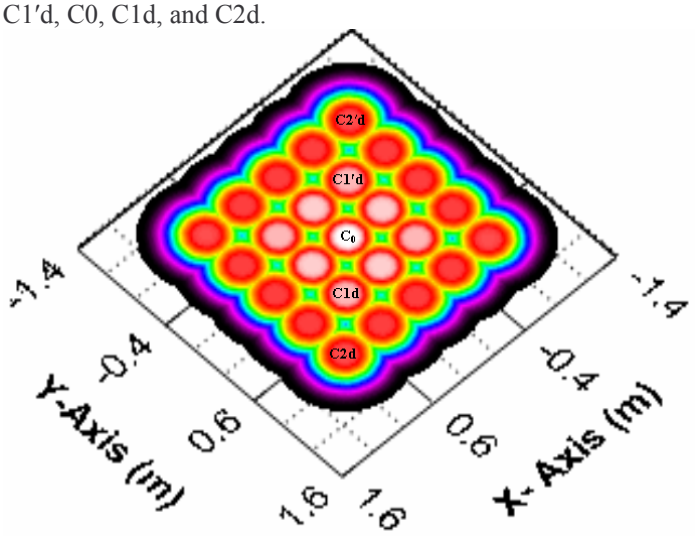

Fig. 4. The top view of the Gaussian profile cells.

We have also simulated the intensity distribution for a 9x9 VCSEL array-based transmitter at a propagation distance of Z = 2.4m. Fig. 5 shows the far-field Gaussian (SG-2) and super-Gaussian (SG-12) intensity distribution for the transmitter across the diagonal cells C4′d C3′d, C2′d, C1′d, C0, C1d, C2d, C3d and C4d. For a 4.2mx4.2m coverage area in the receiver plane, the Gaussian intensity $I_{sg\text{-}2}$ (p=2) as shown in Fig. 5(a) varies from 4.75W/sqm to 82.0W/sqm. This non-uniform intensity profile is converted into uniform flat-top profile for the proposed system using matrix-type DEs as mentioned earlier. Each individual DE converts the non-uniform VCSEL Gaussian beam to a flattop super-Gaussian beam of order *p =12* (SG-12) and directs it to a desired solid angle. For the same coverage area and the propagation distance, the SG intensity $I_{sg\text{-}12}$ as shown in Fig. 5(b) varies from 17.5W/sqm to 49.60W/sqm.

2.4. Receiver Design

Conventional indoor optical wireless systems employ a single element receiver, which consists of an optical concentrator whose output is coupled to a single photodetector. In single element receiver the desired signal, ambient light noise, co-channel interference, and delayed multipath signals are detected together generating single electrical signal. Significant performance improvements can be achieved by using an angle diversity receiver with imaging features [7]. The receiver for the proposed system as shown in Fig. 2(b) can be implemented using imaging mechanism to detect the signals received from different directions. It consists of focusing and imaging optics and a low-capacitance array of InGaAs detectors [8] with a relatively small FOV to reduce shot noise. To make the receiver robust against blockage, its overall FOV is made wide (±45º to ±50º) by using a 9x9 InGaAs-based PIN detector arrays. The detector arrays allow the angle of arrival of the beam to be determined and hence the direction of the required uplink from terminal to the base station. The system is therefore a combination of a tracking transmitter and tracking receiver. The effects of multipath dispersion are minimized due to the use of multiple detector arrays in the receiver. Each element of the detector array uses receiver electronics to track the direction from which the maximum radiation is received.

Selection of Front-end Amplifier Topology

A front-end amplifier called the preamplifier performs the critical function of interfacing the photodiode to the rest of the receiver. Typically, the preamplifier converts the received photo current into a voltage signal. The preamplifier plays a crucial role in determining many aspects of the overall performance of the receiver including speed, sensitivity and dynamic range. Since this amplifier is DC coupled to the photodiode, it must also have a reasonable dynamic range to avoid saturation due to ambient illumination and to accommodate considerable variation in signal power as the link range varies.

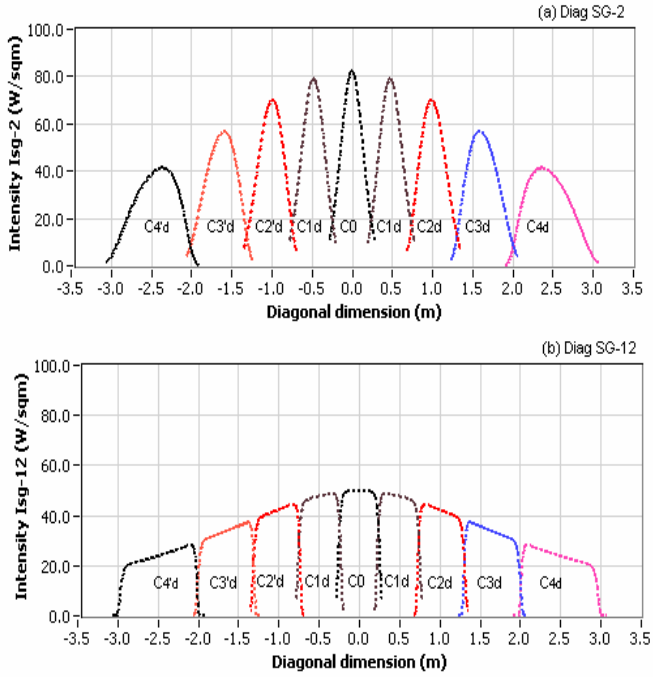

Fig. 5. Simulated intensity distribution of 9x9 VCSEL array based transmitter across the diagonal cells at a propagation distance of 2.4m; (a) Gaussian and (b) super-Gaussian.

Three common amplifier topologies (9) shown in Fig. 6 can be used to perform this function. The high-impedance receiver shown in Fig. 6(a) has a characteristic R_1C_d time constant that is much longer than one bit period, which requires the use of an equalization filter to produce a correct output signal. This topology offers the best noise performance of the three, primarily due to the low noise contribution of the large sense resistor. However, this large sense resistor also causes it to have the lowest dynamic range of the three. In addition, the need for a matched equalization filter makes it more complex than the others. The low-impedance receiver shown in Fig. 6(b) has an R_2C_d time constant that is much shorter than one bit period. This alleviates the need for the equalization filter. Although the small sense resistance leads to the highest dynamic range of the three amplifiers, it also causes it to have the worst noise performance.

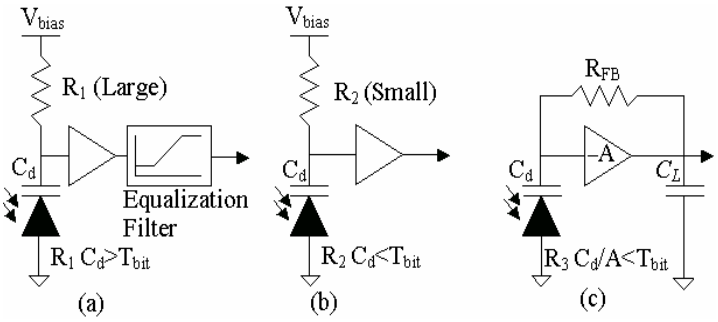

Fig. 6. Topologies of preamplifiers; (a) high-impedance (b) low-impedance and, (c) transimpedance configuration.

The transimpedance amplifier shown in Fig. 6(c) offers a compromise between these two extremes, offering decent dynamic range and noise performance while avoiding the complexity of the high-impedance design. The negative feedback loop offers a simple mechanism to bias the photodiode as well as the core voltage amplifier, further reducing complexity. Further, $R_{FB}C_d$ may be much longer than one bit period without the need for equalizing filters. This allows the use of relatively large feedback resistors to achieve high sensitivity and low noise. These benefits make the transimpedance amplifier the most attractive for the proposed receivers.

SNR Estimator and Best Select Circuit

In the proposed system, the signals from the 9x9 InGaAs-based detector array can be amplified separately by an eighty one-channel transimpedance preamplifier circuit and passed to a signal to noise ratio (SNR) estimator and best selector circuit to permit the selection of the strongest signal. In our system application, the ambient light interference is approximately constant; hence the strongest signal will be the signal with the highest SNR. However, there may be cases where ambient light produces the largest signal. In this case, no data clock will be recovered and this can be used as an indicator that an alternative signal is required. The selected preamplified signal having best SNR is passed to the receiver filter and post-amplifier for the further processing. The processed signal is sent to the clock recovery (synchronization) and decoding/demodulation stages. The SNR estimator and best select circuit also sends control signals to the source enable and control circuit of the transmitter to activate the corresponding VCSEL.

Optical Signal Reception

The optical receiver for the proposed transceiver utilize a focusing and imaging optics known as imaging concentrator that forms an image onto a photodetector in the imaging PIN-photodetector array, each equipped with a separate preamplifier (Fig. 7). The receiver employs an optical filter to attenuate unwanted ambient light. The receiver collects light from some field of view that contains one or more VCSEL beams of the multibeam transmitter oriented towards it. The simulated super-Gaussian intensity distribution I_{sg-12} shown in Fig. 5(b) of all the transmitted VCSEL beams within their convergence angles (cell radii) is nearly uniform. Therefore, the optical power detected by the receiver at an incidence angle ψ (measured with respect to the receiver surface normal) can be given by

$$P_R = I_{sg-12}(r).T_F(\psi).T_C(\psi).A_{img}.\cos\psi \tag{2}$$

where $I_{sg-12}(r)$ is the incidence (super-Gaussian order 12) optical intensity (watt/sqm) in the receiver plane at angle ψ, $T_F(\psi)$ and $T_C(\psi)$ are the transmission factors of optical filter and imaging optics (concentrator) at angle ψ, respectively, and A_{img} (sqm) is the imaging optics area at normal incidence. The value of $T_F(\psi)$ and $T_C(\psi)$ always lie between 0 and 1. The imaging optics should have an acceptance angle ψ_a such that when ψ exceeds ψ_a, the transmission factor $T_C(\psi)$ rapidly approaches zero.
Ideally, all of the detected power given by Eq. (2) is imaged into a single photodetector in the 9x9 photodetector array. If A_{det} is the area of each detector and G is the gain of the imaging optics, then

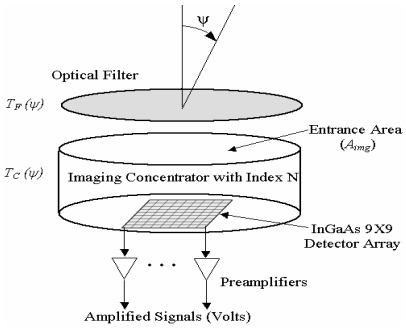

Fig. 7. Imaging receiver, which employs an imaging concentrator and a multiple detector array.

$$G = \frac{A_{img}}{A_{\text{det}}} = \frac{n^2}{\sin^2\psi} \tag{3}$$

where n is the refractive index of the imaging optics.
Putting the value of A_{img} from Eq. (3) to Eq. (2), we get

$$P_R = I_{sg-12}(r).T_F(\psi).T_C(\psi).G.A_{\text{det}}.\cos\psi \tag{4}$$

Thus, the received optical signal current of a photodetector in the detector array can be given by

$$i_{sig} = P_R R \tag{5}$$

where R is the responsivity of the photodetector in A/Watt at the transmission wavelength λ.

Optical Noise and SNR Calculation

The fundamental limiting source of noise in the proposed receivers is the ambient light reflected from the field of view. To calculate the received ambient power, the background scene in the FOV can be modelled as a diffuse Lambertian reflector. Therefore the received ambient power does not depend on the angle of the background surface with respect to the receiver, so we can assume a normal background surface to simplify the calculations.
Thus, the effective ambient optical power incident on the field of view of a detector in the 9x9 detector array is simply

$$P_{BG} = I_{r\,amb}\left(Z.\frac{\theta_r}{N}\right)^2.\Delta\lambda \tag{6}$$

where, $I_{r\ amb}$ is the ambient spectral intensity in W/(sqm.nm) at the transmission wavelength, θ_r is the full FOV of the receiver, N is the total number of detectors in the detector array, and $\Delta\lambda$ is the optical bandwidth of the receiver filter in nm. This will generate a background illumination DC current in each detector and can be given by

$$I_{BG} = \frac{P_{BG}.R_{BG}}{\pi Z^2} A_{img} T_F(\psi).T_C(\psi).R \tag{7}$$

where, R_{BG} is the reflectivity of the background.

The induced DC current will lead to a white shot noise photocurrent (i_{shot}) having the variance

$$\sigma_s^{\ 2} = \langle i_{shot}^{\ 2} \rangle = 2q.I_{BG}.\Delta f \tag{8}$$

where q is the electronic charge and Δf is the effective bandwidth of the receiver.

Now, the SNR of the proposed PIN detector array based receiver can be given by

$$SNR = \frac{I_{sig}^{\ 2}}{\sigma_s^{\ 2}} = \frac{(P_R.R)^2}{2q.I_{BG}.\Delta f} \tag{9}$$

2.5. System Integration

The realization of multibeam VCSEL-array based transmitters and InGaAs-based PIN-photodetector array based imaging receivers using high-performance custom arrays and discrete components is very expensive and power consuming. Modern digital CMOS-smart pixel technology can be used to realize the proposed transceivers. Using this technology, the hybrid integration of VCSELs along with their drivers can be done with CMOS electronics. For the receiver, the photo detection and the detected signal amplification functions can be integrated into every pixel [10] called smart pixel in the array. This type of integration provides an elegant and inexpensive way to achieve high per pixel bit rates. The imaging receivers implemented using this technique will consume only a few mW of total power and are well suited for the proposed application.

2.6. Modulation and Demodulation Scheme

Pulse position modulation (PPM) scheme is widely used in indoor optical wireless links because of its high average–power efficiency. But the performance of PPM is degraded seriously at high bit rates by multipath dispersion. For the proposed system, a slightly modified scheme known as differential pulse position modulation (DPPM) [2] can be used successfully. DPPM offers improved link power budget and bandwidth efficiency. Moreover, for DPPM, phase-locked loop is not required for symbol synchronization.

2.7. Medium Access Control (MAC) Protocol

In wireless networks, the carrier sense multiple access/collision detection (CSMA/CD) protocol [11], which is used with great success in Ethernet, is not very efficient due to interference from neighboring cells, the relatively large amount of time taken to sense the channel, and the hidden node problem. However, the proposed system does not suffer from these problems and can use the CSMA/CD protocol. The transceiver of the base station routes signals to and from the active transceiver pairs of the machines within the coverage. Additionally, the BS can be modified to function as Ethernet switch, where narrow beams will act as ports of Ethernet switch.

3. CONCLUSIONS

In this paper, we have presented the design aspects of high-performance indoor optical wireless transceivers for local area networking. Since the proposed system uses 2-D array of VCSELs emitting at 1.55μm, it is eye-safe, nearly immune to ambient light noise and offers excellent power budget. Moreover, shot noise is reduced by the small field of view of receiver array elements and effects of multipath dispersion are minimized due to the use of multiple detector arrays in the receiver. The links of the proposed transceivers are based on star network topology and the base station at the ceiling establishes a shared medium. Therefore, the links are line-of-site (directed) type and the channel properties are nearly ideal. Hence the Ethernet MAC protocol can be applied.

REFERENCES

1. J.M. Kahn and J.R. Barry, “Wireless Infrared Communications,” *Proceedings of the IEEE*, vol. 85, no. 2, pp. 265-298, February 1997.
2. Chaturi Singh, *et. al,* "Indoor Optical Wireless Systems: Design Challenges, Mitigating Techniques and Future Prospects" *IETE Technical Review*, vol. 21, no. 2, pp. 101-117, March-April 2004.
3. E. B. Zyambo, D. C. O'Brien, G. E. Faulkner, and D. J. Edwards, "Design of a High speed wireless LAN at long wavelengths," presented at Optical Wireless Communications III, Boston, 4214, pp.115-124, 2000.
4. Julian Cheng, Chan-Long Shieh, Wenbin Jiang, and H.C. Lee, “Long-wavelength VCSELs; A new approach based on AlInGaAs quantum wells”, http://www.e2oinc.com/.
5. David J.T.Heatley, *et. al*, “Optical Wireless: The Story So Far", *IEEE Commun. Magazine*, vol. 36, no. 12, pp. 72-74, 1998.
6. Kari Kataja, *et. al*, “Diffractive Optical Elements in Free-space Data Transmission Systems” , *Pro. SPIE Int. Soc. Opt. Engg.* vol. 3951, pp. 94-101, 2000.
7. J.M.Kahn, *et. al*, “Imaging Diversity Receivers for High Speed Infrared Communication", *IEEE Commun. Magazine*, vol. 36, no. 12, pp 88-94, 1998.
8. Ibrahim Kimukin *et. al*, “InGaAs-Based High-Performance p-I-n Photodiodes”, *IEEE Photonics Technology Letters*, vol. 14, no. 3, pp. 366-368, March-2002.
9. Y. E. Tsividis and J. Franca, *“Design of Analog-Digital VLSI Circuits for Telecommunications and Signal* Processing,” Prentice Hall, 1994, Second Edn.
10. Daniel A. Van Blerkom *et. al*, “Transimpedance Receiver Design Optimization for Smart Pixel Arrays”, Journal of Lightwave *Technology,* vol. 16, no. 1, pp. 119-126, 1998.
11. K.C.Chen, “Medium Acces Control of Wireless LANs for Mobile Computing", *IEEE Networks Magazine*, 1994, 8, (5), pp. 50-63.